

Design, synthesis, and biological evaluation of human sialidase inhibitors. Part 1: Selective inhibitors of lysosomal sialidase (NEU1)

Sadagopan Magesh,^{a,*} Setsuko Moriya,^b Tohru Suzuki,^c
Taeko Miyagi,^{b,d} Hideharu Ishida^a and Makoto Kiso^{a,d,*}

^aDepartment of Applied Bioorganic Chemistry, Gifu University, Gifu 501-1193, Japan

^bDivision of Biochemistry, Miyagi Cancer Center Research Institute, Natori, Miyagi 981-1293, Japan

^cLife Science Research Center, Gifu University, Gifu 501-1193, Japan

^dCREST, Japan Science and Technology Corporation (JST), Tokyo, Japan

Received 25 September 2007; revised 12 November 2007; accepted 21 November 2007

Available online 28 November 2007

Abstract—We here report the design and synthesis of selective human lysosomal sialidase (NEU1) inhibitors. A series of amide-linked C9 modified DANA (2-deoxy-2,3-dehydro-*N*-acetylneuraminic acid) analogues were synthesized and their inhibitory activities against all four human sialidases (NEU1–NEU4) were determined. Structure-based approach was used to investigate the basis of selectivity of the compounds with experimentally observed activity. Results from the present study are found to be informative in a qualitative manner for the further design of isoform selective human sialidase inhibitors for therapeutic value.
© 2007 Elsevier Ltd. All rights reserved.

Sialidases (Neuraminidases) contribute to the regulation of many cellular activities by catalyzing the hydrolysis of terminal sialic acid moiety from various oligosaccharides, glycolipids, and glycoproteins. They are widespread in nature, from viruses, microorganisms like bacteria, fungi, and protozoa to higher animals including humans.¹ They are thought to be involved in several biological events such as molecular transport, antigen masking, proliferation, differentiation, transformation, and signal transduction.²

Sialidase is a virulence factor for many pathogens like virus, bacteria, and protozoa.³ To date, sialidase from viral origin has been most extensively studied, which led to structure-based drug discovery of a new class of antiviral agents that specifically target the influenza virus.⁴ Sialidase from the bacteria *Vibrio cholerae* and the *trans*-sialidase from the protozoa *Trypanosoma cruzi* are also considered as potential drug targets for the therapeutic agents against cholera and chagas's disease, respectively.⁵ In humans,

four types of sialidases are known and have been classified based on their subcellular localization, namely the intra lysosomal sialidase NEU1, the cytosolic sialidase NEU2, the plasma membrane-associated sialidase NEU3, and the lysosomal or mitochondrial membrane-associated sialidase NEU4. These isoforms differ in their substrate specificities and physiological functions.⁶

Aberrant expression of human sialidases has been found to be associated with the development of various pathological conditions. In a recent study with NEU1 knock-out mice, reduced IDL and LDL cholesterol levels and decreased atherosclerotic lesions were observed.⁷ NEU3 was found to be significantly up-regulated in various human cancers and its up-regulation was correlated with the apoptosis suppression and the promotion of motility in cancer cells.⁸ Apart from this, NEU3 overexpression in mice developed a diabetic phenotype associated with hyperinsulinemia, islet hyperplasia, and increased β -cell mass.⁹ These studies suggest that they might play important etiological and pathogenic roles in cancer, arteriosclerosis, and diabetes. Furthermore, NEU2 expression was found to induce the apoptosis and was inversely correlated with the metastasis, invasion, and motility.¹⁰ NEU4 has proved to have an important role in the maintenance of normal mucus

Keywords: Sialidase; Inhibitor design; DANA; Selectivity; Homology models; Docking.

* Corresponding authors. Tel.: +81 58 293 2918; fax: +81 58 293 2840; e-mail addresses: sadmag77@gmail.com; kiso@gifu-u.ac.jp

and its down-regulation may contribute to invasive properties of colon cancers, and also found to be associated with mitochondrial apoptosis pathway.¹¹

The differences in the localization and the physiological function of the various isoforms of this enzyme prompted us to use these differences to design inhibitors that could be specific to each of these isoforms. The main objective of our work is ‘*Design in*’ over NEU1 or NEU3 and ‘*Design out*’ of its paralogs to minimize the cross reactivity or potential side effects. In any case, identification of selective inhibitors for individual isoforms can be used as molecular probes for specific functions of human sialidases.

In our previous study we used both sequence and structural information to predict the selectivity-related residues using computational methods. We employed

homology modeling techniques to construct a three-dimensional model structure of sialidases NEU1, NEU3, and NEU4 using the crystal structure of NEU2.¹² The overlay of crystal structure of NEU2–DANA complex with predicted models, and DANA (1) and its four constituent groups required for binding are given in Figure 1. Despite the fact that human NEU isoforms share a high-level amino acid conservation in the active site and its vicinity, they seem to have some striking differences, particularly in the DANA’s glycerol binding group, which could be exploited to design the selective inhibitors. Accordingly, we designed some of the hydrophobic derivatives of DANA modified at glycerol side chain. We began our investigation with some varying hydrophobic groups linked to *N*-amide at C9 position of DANA, thus allowing utilization of steric fit/hindrance principles to probe the selectivity among human isoforms.

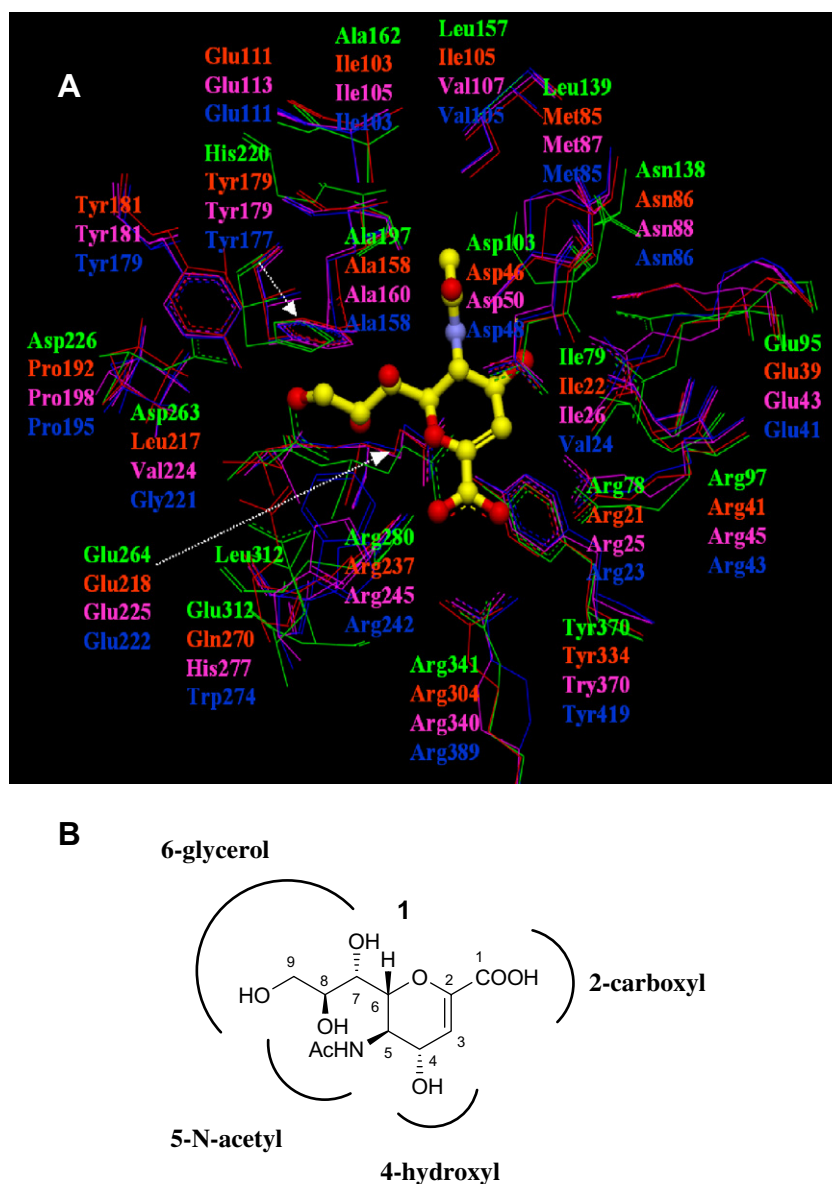
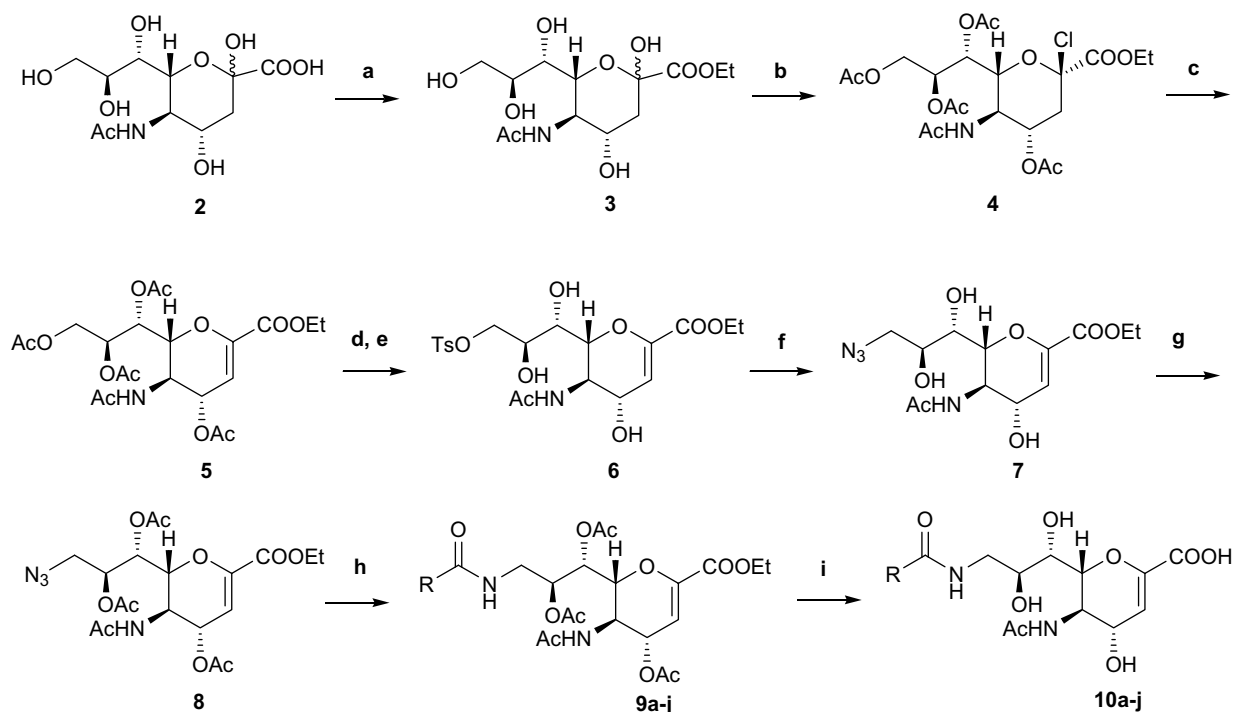


Figure 1. (A) Overlay of the crystal structure of NEU2–DANA complex with predicted models. The active site residues of NEU1, NEU2, NEU3, and NEU4 are colored green, red, pink, and blue, respectively. (B) DANA (1) and its four constituent groups required for binding.



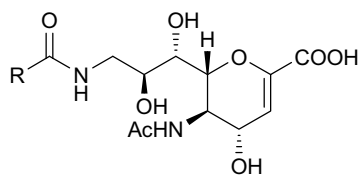
Scheme 1. Reagents and conditions: (a) H^+ resin, EtOH, 50 °C, 1 d; (b) AcCl, rt, 3 d; (c) Et_3N , DCM, rt, o/n (62% over three steps); (d) MeONa, EtOH, rt, o/n (75%); (e) TsCl, pyridine, 0 °C, 1 d (71%); (f) NaN_3 , acetone– H_2O , 70 °C, 2 d (80%); (g) Ac_2O , pyridine, rt, o/n (76%); (h) RCOCl , DPPE, THF, rt, 2–24 h (45–70%); (i) 1—LiOH, MeOH– H_2O –THF, 0 °C, 6 h; 2— H^+ resin (>70%).

Synthetic route to the present series of C9 amide derivatives of DANA is outlined in Scheme 1. Starting material, *N*-acetylneuraminic acid (Neu5Ac) **2**, was esterified with ethanol in the presence of an acidic ion exchange resin to give an ester **3**. This ester was treated with acetyl chloride under neat conditions to afford **4**. Compound **5** was prepared by β -elimination of **4** in the presence of triethylamine as a base. Deprotection of the *O*-acetyl groups in **5** with CH_3ONa , followed by selective tosylation of the primary hydroxyl group using *p*-toluenesulfonyl chloride, provided 9-*O*-tosyl derivative **6**, which was converted to the corresponding azide **7** by the treatment with sodium azide in aqueous acetone. Key intermediate **8** was obtained from **7** in a high yield using excess of acetic anhydride in pyridine. A Staudinger-type reductive acylation of compound **8** with various acid chlorides and DPPE gave the compounds **9a–j** in moderate yields. A small library of these compounds was prepared using a simple parallel synthesizer. Subsequent deprotection of derivatives **9a–j** with LiOH/ H_2O /MeOH gave the target C9 amides of DANA **10a–j** in good yields.¹³

Inhibitory activities of the C9 DANA amides **10a–j** against all four human sialidases were investigated.¹⁴ The IC_{50} values of compounds **10a–j** and DANA (**1**) are given in Table 1. In this series it has been found that the size and the geometry of the alkyl side chains significantly influenced the potency and the selectivity of the compounds toward the different NEU isoforms. The results obtained suggest that the hydrophobic amide derivatives at C9 might be more selective for NEU1 as the other isoforms show a significant reduction (from

low μM to >1000 μM) in their binding affinities in comparison to the reference compound, DANA. The change of linear alkyl groups from methyl **10a**, propyl **10e** to butyl **10h** (58 μM , 32 μM to 10 μM) has steadily increased the potency of NEU1 though the order of magnitude of improvement is low. Replacement of linear chain with cycloalkyl like cyclopropyl **10c** (680 μM) decreased the affinity toward NEU1, whereas cyclopentyl **10d** (135 μM) showed nearly similar activity as DANA. In the case of NEU4, **10a** showed to some extent improved affinity in comparison to other analogues in this series. The replacement of methyl group in **10a** with isopropyl **10g** (>1000 μM) and α -methyl substitution of **10e** to 2-methylpropyl in **10f** (565 μM) also reduced the NEU1 inhibition. Surprisingly, phenyl ring-containing derivative **10b** (13 μM) inhibited NEU1 comparably to **10h**, and showed slightly higher affinity toward human sialidase NEU3 (320 μM) when compared with other derivatives. Sterically bulky and branched alkyl groups like *tert*-butyl **10i** and 2-ethylpropyl **10j** severely diminished the NEU1 inhibitory activity to over 1000 μM range. These data indicate that *n*-butyl analogue **10h** has improved binding affinity (10 μM) to NEU1 with \sim 15-fold improvement over DANA (143 μM), whereas **10h** has decreased binding affinity over a 100-fold toward NEU2, NEU3, and NEU4 (>1000 μM) compared to that of DANA. Taken together, more than a 200-fold selectivity for NEU1 was achieved with **10h** over NEU2, NEU3, and NEU4 with respect to DANA.

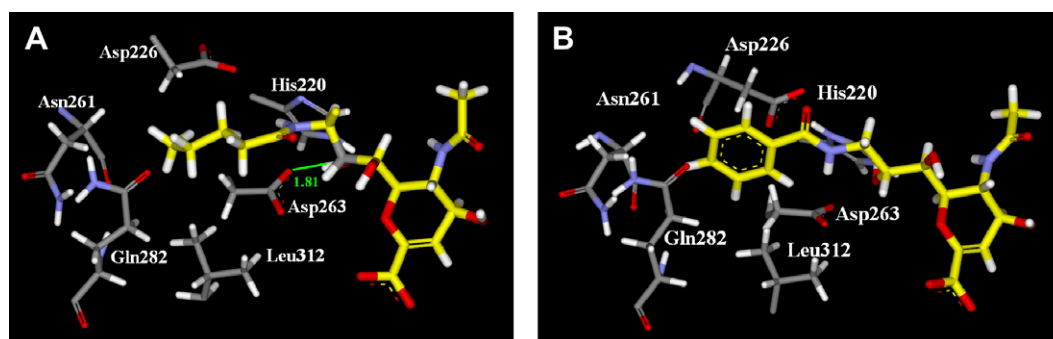
In order to gain further insight into the structural basis of inhibition, we performed the docking studies on the basis of our homology models and the crystal structure

Table 1. Chemical structures of compounds **10a–j** and their inhibitory activities against human sialidases: NEU1, NEU2, NEU3, and NEU4

Compound	R	Sialidase inhibition (IC ₅₀ μM)			
		NEU1	NEU2	NEU3	NEU4
1 (DANA)		143	43	61	74
10a	Methyl	58	>1000	>1000	580
10b	Phenyl	13	865	320	810
10c	Cyclopentyl	135	>1000	>1000	>1000
10d	Cyclopropyl	680	>1000	>1000	825
10e	Propyl	32	>1000	>1000	923
10f	2-Methylpropyl	565	>1000	>1000	>1000
10g	Isopropyl	>1000	>1000	>1000	>1000
10h	<i>n</i> -Butyl	10	>1000	>1000	>1000
10i	<i>tert</i> -Butyl	>1000	>1000	>1000	>1000
10j	2-Ethylpropyl	>1000	>1000	>1000	>1000

of NEU2 (PDB entry 1VCU)¹⁵ using DS LigandFit. LigandFit gives the best poses at the binding site by a stochastic conformational search and by evaluation of the energy of the ligand–protein complex.¹⁶ The compounds **10a–j** were docked into the active site of human sialidase isoforms using DANA as a control ligand.¹⁷ The binding modes of compounds **10a**, **10b**, **10e**, and **10h** are convincing with NEU1, but are apparently in an irrational mode with other isoforms active sites. In our earlier study,¹² we reported that the active site of NEU1 is relatively larger and possesses a different shape and charge distribution as compared to other isoforms, which differ from each other by only two amino acids (Leu217 and Gln270 in NEU2, Val224 and His277 in NEU3, Gly221 and Trp274 in NEU4) proximal to the glycerol side chain of DANA. Even though glycerol binding subsite of NEU1 is majorly composed of acidic amino acids (Asp226, Asn261, Asp263, and Gln282) similar to viral sialidase, the hydrophobic faces of the these amino acid side chains and Leu313 might form a hydrophobic channel in the active site. The docking observations suggest that linear alkyl and phenyl side chains could sterically fit into this channel by forming favorable van der Waals interactions which may ac-

count for their improved binding affinities. The binding pose of C9 substituent of model compounds **10h** and **10b** in NEU1 is shown in Figure 2. It appears that the common Tyr residue (181 in NEU2 and NEU3, 179 in NEU4) is present in the edge of the active site of NEU2–NEU4, sterically preventing the linear, branched or cycloalkyl chains from the binding and this steric clash might force the inhibitors to adopt irrational binding modes. As a result alkyl groups are exposed out into the solvent space, and may contribute to the decrease in their binding affinities towards NEU2, NEU3, and NEU4, and the increased NEU1 selectivity. Interestingly, the binding pose of phenyl analogue **10b** in isoforms other than NEU1 shows π – π stacking against the phenyl ring of the same Tyr residue, which can contribute to the slight improvement in the observed activity as compared to other analogues. Additionally, the docked pose of analogue **10b** in NEU3 shows an extra H-bond with His277 which can explain its increased affinity to NEU3 as compared to NEU2 and NEU4. The docking pose of simple methyl analogue **10a** in NEU4 clearly suggests that the loss of hydrophobic face due to the replacement of Leu217 in NEU2 and Val224 in NEU3 by Gly221 leads to less steric hindrance at the

**Figure 2.** The binding pose of C9 substituent of model compounds **10h** (A) and **10b** (B) in the active site of NEU1 model. Green line represents the hydrogen bonding.

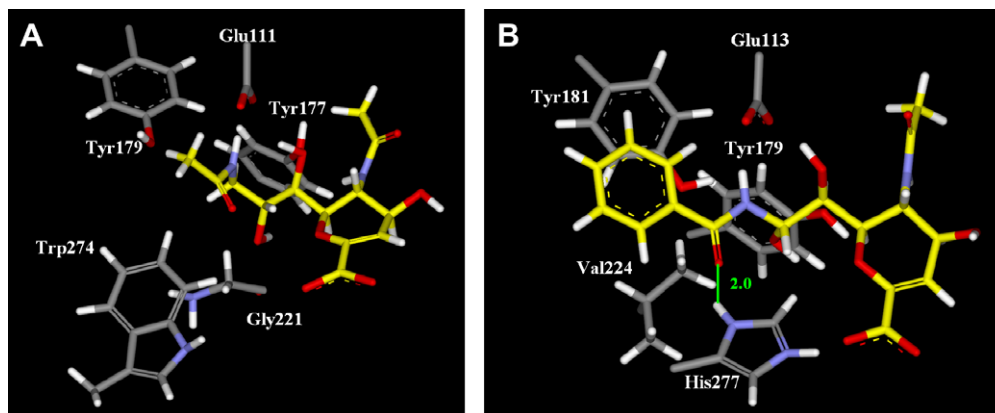


Figure 3. The binding pose of C9 substituent of compound **10a** in NEU4 model (A) and compound **10b** in NEU3 model (B). Green line represents the hydrogen bonding.

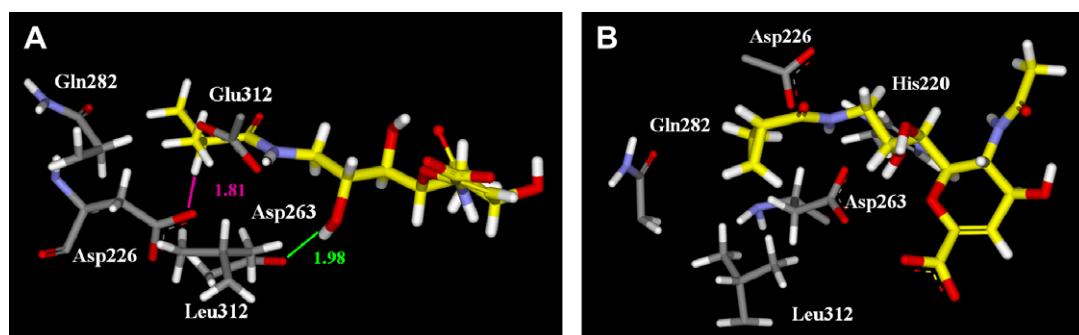


Figure 4. The binding pose of C9 substituent of a branched chain compound **10g** (A) and a cycloalkyl analogue **10c** (B) in the active site of NEU1 Model. Green and pink lines represent the hydrogen bonding and steric clash, respectively.

binding site of NEU4. This can explain the slightly higher affinity of **10a** to NEU4 over NEU2 and NEU3. However, this compound (**10a**) is 10-fold less potent than parent compound DANA **1** for NEU4. The binding pose of C9 substituent of compound **10a** in NEU4 (A) and compound **10b** in NEU3 (B) is shown in Figure 3. These observations strongly imply that C9 substituents of any size are too bulky and inflexible to fit into the active site of NEU2, NEU3, and NEU4 and confer an opportunity for NEU1 selectivity. The binding modes of the branched chain analogues **10f**, **10g**, **10i**, and **10j** suggest that the steric clashing of inhibitors with the side chain of Asp226 in NEU1 can abolish their binding affinity toward NEU1. Although the interacting poses of cycloalkyl analogues **10c** and **10d** in NEU1 are seemingly favorable, probably their conformational rigidity could be a reason for the reduced binding affinity. The binding pose of C9 substituent of isopropyl analogue **10g** and cyclopropyl analogue **10c** in NEU1 is shown in Figure 4. On the whole, our docking studies clearly reveals a reasonable correlation between the experimental IC_{50} values of the inhibitors with their predicted binding poses and further suggest that differences in the active site topology of human sialidases might impart the selectivity to the inhibitors.

In summary, we report here some C9 amide-linked hydrophobic derivatives of DANA as selective human lysosomal sialidase (NEU1) inhibitors. To the best of

our knowledge, this is the first report of structure-based design of selective human sialidase inhibitors. The efforts to integrate structural information with inhibitor activity were actively pursued. The results obtained in the present study are thought to be important for our continuing research efforts in the design and synthesis of isoform selective human sialidase inhibitors for therapeutic value. The synthesis and optimization of molecular probes in this regard are ongoing, and the results will be reported in due course.

Acknowledgments

The first author (S.M.) is grateful to Ministry of Education, Culture, Sports, Science and Technology, Government of Japan (MEXT), for the financial support, No. 042271. This work was supported in part by Grants-in-Aid (No. 17101007) for Scientific Research from MEXT and by CREST of JST (Japan Science and Technology Corporation) to M.K. The authors are thankful to Ms. Subashree and Ms. Savita for many valuable discussions during preparation of the manuscript.

References and notes

1. Monti, E.; Preti, A.; Venerando, B.; Borsani, G. *Neurochem. Res.* **2002**, *27*, 649.

2. Achyuthan, K. E.; Achyuthan, A. M. *Comp. Biochem. Physiol. B: Biochem. Mol. Biol.* **2001**, *129*, 29.
3. Rosenberg, A.; Schengrund, C.-L. In *Biological Roles of Sialic Acid*; Rosenberg, A., Schengrund, C.-L., Eds.; Plenum: New York, 1976; pp 295–359.
4. von Itzstein, M.; Wu, W. Y.; Kok, G. B.; Pegg, M. S.; Dyason, J. C.; Jin, B.; Phan, T. V.; Smythe, M. L.; White, H. F.; Oliver, S. W.; Colman, P. M.; Varghese, J. N.; Ryan, D. M.; Woods, J. M.; Bethell, R. C.; Hotham, V. J.; Cameron, J. M.; Penn, C. R. *Nature* **1993**, *363*, 418.
5. (a) Mann, M. C.; Thomson, R. J.; Dyason, J. C.; McAtamney, S.; von Itzstein, M. *Bioorg. Med. Chem.* **2006**, *14*, 1518; (b) Neres, J.; Bonnet, P.; Edwards, P. N.; Kotian, P. L.; Buschiazio, A.; Alzari, P. M.; Bryce, R. A.; Douglas, K. T. *Bioorg. Med. Chem.* **2007**, *15*, 2106.
6. Miyagi, T.; Kato, K.; Ueno, S.; Wada, T. *Trends Glycosci. Glycotechnol.* **2004**, *16*, 371.
7. (a) Yang, A. E.; Tedesco, V.; Kufaiishi, H. F.; Trigatti, B. L.; Igdoura, S. A. *Atheroscler. Suppl.* **2006**, *7*, 488; (b) Igdoura, S. A.; Yang, A.; DeSA, D.; Trigatti, B. L. *Atheroscler. Suppl.* **2007**, *8*, 187; (c) Igdoura, S. A.; Trigatti, B. L. U.S. Patent Application 20070074300, 2007.
8. (a) Kakugawa, Y.; Wada, T.; Yamaguchi, K.; Yamanami, H.; Ouchi, K.; Sato, I.; Miyagi, T. *Proc. Natl. Acad. Sci. U.S.A.* **2002**, *99*, 10718; (b) Nomura, H.; Tamada, Y.; Miyagi, T.; Suzuki, A.; Taira, M.; Suzuki, N.; Susumu, N.; Irimura, T.; Aoki, D. *Oncol. Res.* **2006**, *16*, 289; (c) Ueno, S.; Saito, S.; Wada, T.; Yamaguchi, K.; Satoh, M.; Arai, Y.; Miyagi, T. *J. Biol. Chem.* **2006**, *281*, 7756; (d) Wada, T.; Hata, K.; Yamaguchi, K.; Shiozaki, K.; Koseki, K.; Moriya, S.; Miyagi, T. *Oncogene* **2007**, *26*, 2483.
9. Sasaki, A.; Hata, K.; Suzuki, S.; Sawada, M.; Wada, T.; Yamaguchi, K.; Obinata, M.; Tateno, H.; Suzuki, H.; Miyagi, T. *J. Biol. Chem.* **2003**, *278*, 27896.
10. (a) Miyagi, T.; Wada, T.; Yamaguchi, K.; Hata, K. *Glycoconj. J.* **2004**, *20*, 189; (b) Tringali, C.; Lupo, B.; Anastasia, L.; Papini, N.; Monti, E.; Bresciani, R.; Tettamanti, G.; Venerando, B. *J. Biol. Chem.* **2007**, *282*, 14364.
11. (a) Yamaguchi, K.; Hata, K.; Koseki, K.; Shiozaki, K.; Akita, H.; Wada, T.; Moriya, S.; Miyagi, T. *Biochem. J.* **2005**, *390*, 85; (b) Yamanami, H.; Shiozaki, K.; Wada, T.; Yamaguchi, K.; Uemura, T.; Kakugawa, Y.; Huijiya, T.; Miyagi, T. *Cancer Sci.* **2007**, *98*, 299.
12. Magesh, S.; Suzuki, T.; Miyagi, T.; Ishida, H.; Kiso, M. *J. Mol. Graph. Model.* **2006**, *25*, 196.
13. All new compounds gave the satisfactory spectroscopic and analytical data.
14. *Sialidase inhibition assay*: Inhibitory activities were evaluated using the homogenates obtained from HEK-293 cells transiently transfected with the expression plasmid containing full-length human sialidase cDNA. For NEU1 expression, a protective protein cDNA was co-transfected with NEU1 cDNA. Assays were performed using 4MU-NeuAc (NEU1, NEU2, and NEU4) or mixed gangliosides (NEU3) as a substrate. One unit (nmol/h) of the enzyme was incubated for 30–60 min for each assay. Each compound was tested at four different mM concentrations (0.05, 0.1, 0.5, and 1) and IC₅₀ values from concentration-inhibition curves were calculated by means of non-linear regression analysis using Microsoft Excel.
15. Chavas, L. M.; Tringali, C.; Fusi, P.; Venerando, B.; Tettamanti, G.; Kato, R.; Monti, E.; Wakatsuki, S. *J. Biol. Chem.* **2005**, *280*, 469.
16. Venkatachalam, C. M.; Jiang, X.; Oldfield, T.; Waldman, M. *J. Mol. Graph. Model.* **2003**, *21*, 289.
17. *Docking analysis*: All docking calculations were performed using LigandFit algorithm, which is implemented in DS modeling 1.5, Accelrys Inc., San Diego, USA (www.accelrys.com). Docking was performed in two-step process. First, the active site was defined as a subset that contains residues in which any atom lies within 8.0 Å from the DANA. The defined active site was expanded to accommodate the shapes of test compounds by adding extra grid points. Then compounds **10a–j** were flexibly docked into active site of human sialidase models and into the crystal structures of NEU2. Test compounds were built and processed before docking by defining bond orders and charges correctly. In the docking preferences, the number of Monte Carlo trials was set to a fixed value of 5000 and the maximum number of saved poses to 10. Dreiding force field was selected for the grid energy preferences and conjugate gradient method was used for energy minimization. The docked poses were manually checked for their geometrical and electronic matching quality.